

Stabilised Nonlinear Inverse Diffusion for Approximating Hyperbolic PDEs

Michael Breuß¹, Thomas Brox², Thomas Sonar¹, Joachim Weickert²

¹ Technical University Brunswick, Computational Mathematics,
Pockelsstraße 14, 38106 Brunswick, Germany
{m.breuss, t.sonar}@tu-bs.de
www.icm.tu-bs.de

² Mathematical Image Analysis Group, Faculty of Math. and Computer Science,
Saarland University, Building 27, 66041 Saarbrücken, Germany
{brox, weickert}@mia.uni-saarland.de
www.mia.uni-saarland.de

Abstract. Stabilised backward diffusion processes have shown their use for a number of image enhancement tasks. The goal of this paper is to show that they are also highly useful for designing shock capturing numerical schemes for hyperbolic conservation laws. We propose and investigate a novel flux corrected transport (FCT) type algorithm. It is composed of an advection step capturing the flow dynamics, and a stabilised nonlinear backward diffusion step in order to improve the resolution properties of the scheme. In contrast to classical FCT procedures, we base our method on an analysis of the discrete viscosity form. This analysis shows that nonlinear backward diffusion is necessary. We employ a slope limiting type approach where the antidiffusive flux determined by the viscosity form is controlled by a limiter that prohibits oscillations. Numerical experiments confirm the high accuracy and shock capturing properties of the resulting scheme. This shows the fruitful interaction of PDE-based image processing ideas and numerical analysis.

1 Introduction

Starting with Rudin's Ph.D. thesis in 1987 [18], many ideas from computational fluid dynamics and the numerics of hyperbolic conservation laws have entered the field of image processing. Because problems of fluid dynamics and hyperbolic conservation laws involve the formation of shocks, sophisticated numerical methods such as total variation diminishing (TVD) and essentially non-oscillatory (ENO) schemes had to be devised to give a sharp resolution at shocks and to avoid visible numerical oscillations [8, 9, 13]. On the image processing side, image edges carry important information and may be regarded as shocks as well. Often edges are blurred, so it is natural to apply shock-enhancing concepts from computational fluid dynamics. This has led to PDE formulations of shock filters [14] and to stabilised linear backward diffusion [15]; see Fig. 1 for an example. In case that noise is present as well, one aims at preserving or

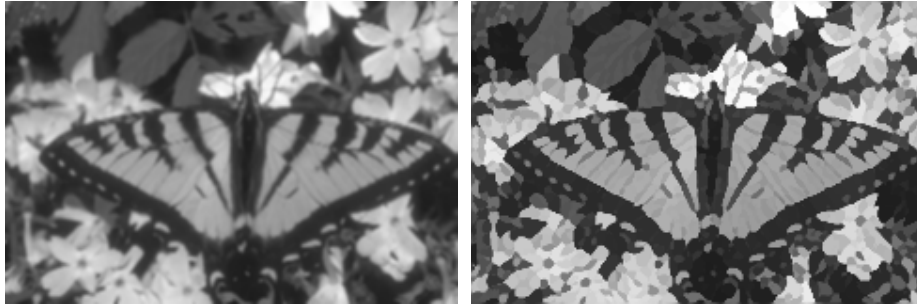


Fig. 1. Left: Original image with blurred edges. **Right:** Image sharpened with stabilized linear backward diffusion [15].

enhancing edges, while simultaneously smoothing at more homogeneous regions. Combinations of shock filtering with mean curvature motion [1] and in particular nonlinear diffusion filtering [16] are suitable concepts to achieve this goal. Interesting variants of nonlinear diffusion include stabilised inverse diffusion equations (SIDEs) [17] and so-called forward-and-backward (FAB) diffusion [7] that explicitly uses negative diffusivities in a certain gradient range. Last but not least, total variation minimisation [19] has been proposed as a variational framework for discontinuity-preserving denoising.

While numerical ideas for hyperbolic conservation laws had undoubtedly a strong impact on modern image analysis, fertilisation in the inverse direction – where image processing methods are applied to improve the numerics of hyperbolic conservation laws – have started only recently: in [10, 11] different variants of numerical schemes are proposed that combine the second-order Lax-Wendroff scheme with anisotropic diffusion filtering with a diffusion tensor [23]; see also [22] for related ideas. All these strategies start with a hyperbolic scheme that gives sharp shock resolution, but suffers from oscillations in the shock areas. Anisotropic diffusion regards such oscillations as noise at edges that can be removed by smoothing along the edge.

On the other hand, there are also monotone first order schemes for hyperbolic conservation laws that do *not* produce oscillations at shocks. Unfortunately, they suffer from strong blurring effects (dissipation) since they involve a significant amount of numerical diffusion (viscosity) to achieve their favourable stability properties. However, if one takes such a scheme as starting point, an interesting question would be if there are useful ideas inspired from edge-enhancing PDE-based image processing that allow to sharpen these shocks. Ideally they should also turn the first order basis method having low accuracy into a higher accurate second-order method without introducing oscillations. For simplicity we focus on the one-dimensional scalar case. We will see that the resulting methods can be regarded to belong to the class of flux-corrected transport (FCT) schemes [2], but in contrast to classical FCT schemes they offer the advantage that they are also applicable to the important class of *nonlinear* conservation laws. It turns out that the appropriate sharpening process from image processing must be a stabilised nonlinear inverse diffusion step. It resembles the stabilised linear inverse diffusion filter that has been proposed by Osher and Rudin [15] for deblurring images.

Our paper is organised as follows: in Section 2 we describe a classical Upwind scheme and analyse its intrinsic numerical diffusion, while Section 3 gives an introduction to FCT schemes. This analysis forms the basis for our novel image-processing inspired FCT scheme that we present in Section 4. Its stability properties are analysed in Section 5. Section 6 presents experiments with linear and nonlinear test scenarios where we compare our method with a state-of-the-art shock capturing scheme: a TVD method with van Leer flux limiter. We conclude our paper with a summary in Section 7.

2 The Classical Upwind Scheme and its Numerical Diffusion

In this paper, we deal with the numerical approximation of hyperbolic conservation laws of type

$$u_t + (f(u))_x = 0, \quad (1)$$

where $u := u(x, t)$ is a scalar-valued function of a one-dimensional space variable x and time t , subscripts denote partial derivatives, and the flux function f is supposed to satisfy $f'(\cdot) \geq 0$.

The underlying method for our novel FCT technique in the next section is the classical *Upwind scheme*

$$U_j^{k+1} = U_j^k - \lambda (f_j^k - f_{j-1}^k). \quad (2)$$

Thereby, we use as in the following the notation U for discrete data in contrast to the sought solution u , and we denote the ratio of mesh parameters as $\lambda = \Delta t / \Delta x$. The upper index k in U_j^k denotes as usual the temporal level $k\Delta t$ while analogously the lower index j denotes the spatial mesh point $j\Delta x$. For shortness of notation, we abbreviate

$$f_j^k := f(U_j^k).$$

Unless stated otherwise, we consider all occurring methods to be stable under the usual CFL condition, see e.g. [13] for details concerning this notion.

One desirable property of the Upwind scheme consists of the fact that the scheme does not produce numerical oscillations:

Proposition 1 (Extrema Diminishing Properties of the Upwind Scheme).

The Upwind scheme (2) is a generalised monotone scheme in the sense of LeFloch and Liu [12], i.e., it is a local extremum diminishing (LED) scheme, while it also does not introduce new extrema during a computation, i.e., it diminishes also the number of extrema (NED property).

Proof. The validity of the assertion follows since under a CFL condition

$$U_j^{k+1} \in \text{conv}(U_{j-1}^k, U_j^k)$$

always follows, where conv denotes the convex hull. (Compare the *data compatibility* notion due to Roe [20].) ♣

Unfortunately, the Upwind scheme also has a severe disadvantage: it suffers from undesirable blurring effects (dissipation). To quantify these viscous artifacts we write the scheme (2) in its *viscous form*, i.e.,

$$U_j^{k+1} = \underbrace{U_j^k - \frac{\lambda}{2} (f_{j+1}^k - f_{j-1}^k)}_{(A)} + \underbrace{\frac{Q_j^{+,k}}{2} (U_{j+1}^k - U_j^k) - \frac{Q_j^{-,k}}{2} (U_j^k - U_{j-1}^k)}_{(B)}. \quad (3)$$

The underlying idea behind this decomposition is to consider part (A) as a second order approximation of (1) in space (and first order in time), while part (B) is (in leading order) the discrete counterpart of the numerical diffusion incorporated in the method (2).

One easily verifies that (2) and (3) can be made identical by choosing viscosity coefficients Q_j^+ and Q_j^- that satisfy

$$Q_j^{+,k} = \lambda \frac{f_{j+1}^k - f_j^k}{U_{j+1}^k - U_j^k} \quad \text{and} \quad Q_j^{-,k} = \lambda \frac{f_j^k - f_{j-1}^k}{U_j^k - U_{j-1}^k}. \quad (4)$$

for $U_{l+1}^k \neq U_l^k$, $l \in \{j, j-1\}$. Note that our assumption $f'(\cdot) \geq 0$ ensures that the viscosities Q_j^\pm are nonnegative. Since the viscosities are proportional to the diffusion coefficients it follows that forward diffusion takes place. This numerical diffusion is responsible for the undesirable blurring effects that are observed with this first-order method. We observe that, in spite of the simplicity of the Upwind scheme, an inherent diffusion process with nonlinear (!) viscosities Q_j^\pm is involved. These nonlinear viscosities are inversely proportional to the derivative of u . In this respect they closely resemble the diffusivities in TV denoising of images [19].

3 FCT Schemes

A common method to compensate for the before mentioned blurring artifacts is the *flux corrected transport* (FCT) algorithm of Boris and Book [2]: a numerical scheme with much numerical diffusion used as a predictor for the evolution is corrected by an antidiffusive step. This principle is used as a basis of many successful FCT type algorithms, see especially [24] and the references therein.

The classical FCT approach as described in [2] is motivated by the method of the *modified equation*: the numerical diffusion incorporated in the predictor step is computed by means of the differential advection-diffusion-equation that the viscous predictor scheme actually approximates with second order accuracy. The resulting diffusion coefficient is annihilated by the antidiffusive step while a limiting procedure ensures that no oscillations develop. For more information on the modified equation, see e.g. the books [8, 13]. The described strategy can be refined by considering an analysis of wave coefficients in the linear case, ensuring especially for linear advection problems a high approximation quality; see [3, 4].

In order to describe the classical FCT method based on the Upwind scheme we use the following data notions:

- $U_j^{k+1/2}$ for the data obtained with the Upwind scheme starting from U_j^k
- U_j^{k+1} for the data obtained after the antidiffusive step.

Let us define the abbreviate notion

$$\Delta U_{j+1/2}^k := U_{j+1}^k - U_j^k. \quad (5)$$

Then the traditional FCT approach amounts to an *antidiffusion step* realised via

$$U_j^{k+1} = U_j^{k+1/2} - g_{j+1/2} + g_{j-1/2} \quad (6)$$

where the fluxes g are chosen in a fashion such that the following directive holds:

Construction Principle 1 (Boris and Book [2]) .

“No antidiffusive flux transfer of mass can push the density value at any grid point beyond the density value at neighboring points.”

The traditional FCT scheme realises this principle by setting

$$g_{j+1/2} := \text{minmod} \left(\Delta U_{j-1/2}^{k+1/2}, \eta_{j+1/2} \Delta U_{j+1/2}^{k+1/2}, \Delta U_{j+3/2}^{k+1/2} \right) \quad (7)$$

where

$$\text{minmod}(a, b, c) := \text{sgn}(b) \max \left(0, \min(\text{sgn}(b)a, |b|, \text{sgn}(b)c) \right) \quad (8)$$

and

$$\eta_{j+1/2} := \frac{\lambda}{2} \bar{a} (1 - \lambda \bar{a}), \quad (9)$$

with \bar{a} determined by

$$\bar{a} := \max_{U \in \text{conv}(U_j^{k+1/2}, U_{j+1}^{k+1/2})} |f'(U)|.$$

Note that (9) is equivalent to Δt times the discrete version of the viscous term of the modified equation obtained by using a local linearisation of (1).

4 A New FCT Scheme with Nonlinear Inverse Diffusion

Let us now introduce a novel variant of FCT schemes that incorporates image processing ideas on stabilised inverse diffusion. In contrast to the previous section, our considerations are based solely on the viscosity form (3). This is a new feature of possible FCT algorithms. Our method of derivation can be advantageous concerning a rigorous analysis of the combined method, especially with respect to the nonlinear case.

A naive step to achieve inverse diffusion would consist of applying a direct antidiffusion process to the predicted data $U^{k+1/2}$ from the Upwind scheme by setting

$$\tilde{g}_{j+1/2} := \frac{1}{2} Q_j^{+,k+1/2} \Delta U_{j+1/2}^{k+1/2}. \quad (10)$$

It is immediately clear that such an antidiffusive step without a direct minmod-type stabilisation as used in (7) may introduce many oscillations. Thus, we limit the antidiffusive flux \tilde{g} from (10) by

$$g_{j+1/2} := \text{minmod}(\tilde{g}_{j-1/2}, \tilde{g}_{j+1/2}, \tilde{g}_{j+3/2}) \quad (11)$$

using the minmod function (8).

The discrete inverse diffusion employed here is similar to an image enhancement algorithm due to Osher and Rudin [15]. However, while the filter of Osher and Rudin is the stabilised inverse filter to *linear* diffusion, we extend this algorithm to be the stabilised inverse filter to *nonlinear* diffusion.

5 Stability Analysis

We are now ready to prove the following stability assertion.

Lemma 1 (Local Extremum Principle).

Let

$$\text{sign}(\Delta U_{j+1/2}^{k+1/2}) = \text{sign}(\Delta U_{j-1/2}^{k+1/2}) \neq 0 \quad (12)$$

hold. Then the FCT scheme defined by

$$U_j^{k+1} = U_j^{k+1/2} - g_{j+1/2} + g_{j-1/2} \quad (13)$$

using g from (11) satisfies locally a discrete minimum–maximum principle.

Proof. The aim is to show that

$$U_j^{k+1} \in \text{conv}(U_{j-1}^{k+1/2}, U_j^{k+1/2}, U_{j+1}^{k+1/2})$$

holds. We only consider the situation defined by

$$\left| U_j^{k+1/2} - U_{j-1}^{k+1/2} \right| \leq \left| U_{j+1}^{k+1/2} - U_j^{k+1/2} \right|, \quad (14)$$

the other case can be treated analogously.

For simplicity, we omit the superscript $k+1/2$ in the following computations. The idea is, starting from (13), to derive the estimate

$$\left| -g_{j+1/2} + g_{j-1/2} \right| \leq |U_j - U_{j-1}|$$

since then the sought convex hull condition is satisfied. Thus, we compute using the Lipschitz continuity of f and a corresponding Lipschitz constant L

$$\begin{aligned}
 & \left| -g_{j+1/2} + g_{j-1/2} \right| \\
 & \leq \left| g_{j+1/2} \right| + \left| g_{j-1/2} \right| \\
 & \stackrel{(11)}{\leq} \left| \frac{1}{2} Q_j^+ \Delta U_{j-1/2} \right| + \left| \frac{1}{2} Q_j^+ \Delta U_{j-1/2} \right| \\
 & \stackrel{(4)}{=} \lambda \left| \frac{f_j - f_{j-1}}{U_j - U_{j-1}} \right| \left| U_j^k - U_{j-1}^k \right| \\
 & = \lambda \left| f_j - f_{j-1} \right| \\
 & \leq \lambda L \left| U_j - U_{j-1} \right| \\
 & \leq \left| U_j - U_{j-1} \right|
 \end{aligned}$$

by the CFL condition. ♣

Because of the properties of the minmod function, the core of the proof also works without the assumption (12). Thus we can give directly

Corollary 1 (Global Extremum Principle).

The investigated scheme satisfies locally and globally a discrete minimum–maximum principle.

It is also possible to prove in the same fashion as in Lemma 1 directly the validity of the NED property if we restrict the time step size such that

$$\Delta t \max_{U \in \mathcal{I}} |f'(U)| \leq \frac{\Delta x}{2},$$

where \mathcal{I} is the relevant range of data values. However, the resulting scheme is in practice quite viscous.

Concerning the approximation of the entropy solution, it is clear by the properties of the underlying Upwind scheme that shocks are approximated at the correct position as long as the data feeding the shock are arranged as a plateau: in this case, the antidiffusive flux becomes zero at the edge of the plateau, leaving at the shock location the Upwind method which propagates the right amount of mass into the shock. The situation becomes more difficult if the data are not arranged in this fashion. This is subject of current investigation.

6 Numerical Experiments

Our tests consist of an *order test* using the approximation of a linear equation with smooth initial condition as well as of *two nonlinear test cases*, where we consider the approximation of a square-wave solution of Burgers' equation and the numerical solution of a Riemann problem for the Buckley-Leverett equation.

Let us stress that the linear advection equation and Burgers' equation can be seen as simple test cases for systems of equations with linearly degenerate and genuinely nonlinear characteristic fields, respectively [9]. The Buckley-Leverett equation imposes the considerable difficulty to approximate a mixed wave solution.

Linear Advection - The Order Test

The order test uses the linear advection equation

$$u_t + u_x = 0$$

propagating smooth initial data

$$u_0(x) = \sin(\pi x)$$

on a grid over $[-1, 1]$ with periodic boundary conditions. We choose a very small time step size, i.e., $\Delta t = 0.0001$, and investigate the error in the L_1 -Norm for a sequence of spatial grids with diminishing mesh widths Δx . The time at which we evaluate the arising sequence of errors is set fixed, i.e., we measure after one revolution after which the analytical solution exactly matches the initial condition. The quantity of interest is the *experimental order of convergence* EOC defined by

$$EOC := \frac{\log(e_{\Delta x}/e_{\Delta x/2})}{\log(2)},$$

where $e_{\Delta x}$ is the L_1 -error measured using the spatial mesh with the parameter Δx . The exact setup and the results of the computations together with the corresponding EOC can be found in Tab. 1. The results show that the inverse diffusion turns the classical Upwind scheme from first order to nearly second order, from which we deduce the sought high resolution property.

# nodes	DX	DT	time steps	L_1 -error $e_{\Delta x}$	EOC
20	0.1	0.0001	20000	0.394969	-
40	0.05	0.0001	20000	0.135555	1.54286
80	0.025	0.0001	20000	0.0508049	1.41584
160	0.0125	0.0001	20000	0.0147794	1.78138
320	0.00625	0.0001	20000	0.00460051	1.68372

Table 1. Arrangement of the computational parameters for the numerical convergence study together with the corresponding L_1 -error and the experimental order of convergence (EOC).

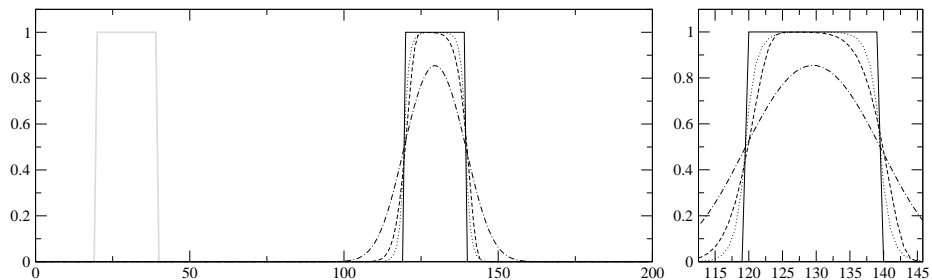


Fig. 2. Linear advection. **Left:** Grey line: initial condition. Solid line: correct solution after $t = 100$. Dotted line: Upwind with antidiffusion. Dashed line: TVD method. Dash-dotted line: Upwind without antidiffusion. **Right:** Zoom.

Fig. 2 depicts a comparison of our scheme to the Upwind scheme without antidiffusion as well as a contemporary TVD method with van Leer limiter, see e.g. [8, 13]. The corresponding numerical solutions are displayed together with the exact solution and the initial condition. The computational parameters have been set to $\Delta t = 0.5$ and $\Delta x = 1$.

Let us note here that there is a wide variety of possibilities to obtain higher order accuracy in standard TVD schemes, for instance flux limiting, slope limiting, or ENO schemes, compare again [8]. We choose here to compare our method with a slope limiter method since this is arguably the simplest and most efficient choice. Concerning the numerical results, no large difference using either method is to be expected with respect to our example.

It can be observed that the proposed FCT-like scheme yields approximately the same accuracy as the TVD method, which supports the order test. When compared to the Upwind scheme without antidiffusion, the antidiffusion step clearly reveals its impact.

Burgers' Equation

A nonlinear test problem is concerned with Burgers' equation

$$u_t + \left(\frac{1}{2}u^2\right)_x = 0$$

supplemented by the initial condition

$$u_0(x) = \begin{cases} 1 & : 20 \leq x < 40 \\ 0 & : \text{else} \end{cases}.$$

This square wave decays to an N-wave like every solution of Burgers' equation. Thus the example has a profound meaning, see e.g. [6, 13] for discussions.

The computational parameters are the same as in the linear example before, and we compute the solution at $t = 100$. We compare again the numerical solutions obtained by the Upwind scheme with and without antidiffusion, as well as the TVD method.

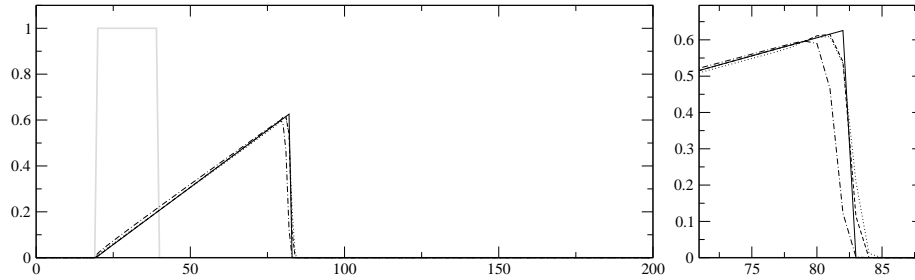


Fig. 3. Burgers equation. **Left:** Grey line: initial condition. Solid line: correct solution after $t = 100$. Dotted line: Upwind with antidiffusion. Dashed line: TVD method. Dash-dotted line: Upwind without antidiffusion. **Right:** Zoom.

The corresponding numerical solutions together with the exact solution are displayed in Fig. 3. For better comparison, a detailed cutout of the region around the shock is depicted beside. Again it can be seen that the proposed scheme yields results very close to those of the TVD method. Note that in this nonlinear case, the classical FCT scheme is not applicable anymore without additional considerations.

Buckley-Leverett Equation

A second nonlinear and even non-convex test problem is based on the Buckley-Leverett equation

$$u_t + \left(\frac{u^2}{u^2 + \frac{1}{2}(1-u)^2} \right)_x = 0$$

supplemented by a Riemann problem as initial condition:

$$u_0(x) = \begin{cases} 1 & : 0 \leq x < 50 \\ 0 & : \text{else} \end{cases} .$$

With the same settings as in the tests before, we obtain the numerical solutions depicted in Fig. 4. The outcome is similar to the experiments before: while the scheme with nonlinear antidiffusion is very close to the TVD scheme, there is quite some difference to the Upwind scheme without antidiffusion, although this difference is smaller than in the other experiments.

7 Conclusions

We have presented a novel FCT-type algorithm for hyperbolic conservation laws. It incorporates stabilised nonlinear inverse diffusion in order to improve the shock resolution of a first-order Upwind scheme. The nonlinear inverse diffusion step is inspired from a stabilised linear inverse diffusion filter that has been proposed by Osher and Rudin for deblurring images. In contrast to classical FCT methods, our scheme arises naturally from the viscosity form of the basic scheme. As a consequence it also applies

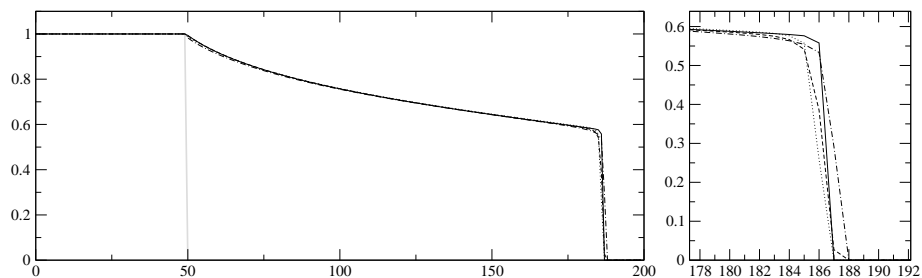


Fig. 4. Buckley-Leverett equation. **Left:** Grey line: initial condition. Solid line: correct solution after $t = 100$. Dotted line: Upwind with antidiffusion. Dashed line: TVD method. Dash-dotted line: Upwind without antidiffusion. **Right:** Zoom.

to the important class of nonlinear problems, even if the flux function is nonconvex. A theoretical analysis has shown that the novel scheme satisfies a global extremum principle and other desirable stability properties, while experiments with linear and nonlinear test scenarios indicate that it has approximately second order accuracy properties. It gives far better results than its underlying Upwind scheme and – in spite of its simplicity – it is even competitive to modern TVD methods for shock capturing approximations of hyperbolic PDEs. Its simplicity accounts for expectations that the method may be better accessible to theoretical analysis than TVD methods. In our ongoing work we further intend to analyse generalisations to the higher dimensional case as well as to systems of conservation laws.

Our work has shown that the connection between numerical schemes for hyperbolic conservation laws and image enhancement methods is not a one-way road: in the meantime, many PDE-based image enhancement techniques have reached a degree of maturity such that they may be highly useful for a number of problems outside the field of image analysis. It is our goal to investigate more of these fascinating interdisciplinary connections in the future.

Acknowledgements

The authors gratefully acknowledge the financial support of their work by the *Deutsche Forschungsgemeinschaft (DFG)* under the grants No. SO 363/9-1 and WE 2602/1-2.

References

1. Alvarez L. and Mazorra L. (1994): Signal and image restoration using shock filters and anisotropic diffusion. *SIAM J. Num. Math.* **31**, pp. 590–605
2. Boris, J.P. and Book, D.L. (1973): Flux corrected transport. I. SHASTA, a fluid transport algorithm that works. *J. Comp. Phys.* **11**, No. 1, pp. 38-69
3. Boris, J.P., Book, D.L. and Hain, K. (1975): Flux corrected transport II: Generalizations of the method. *J. Comp. Phys.* **18**, pp. 248-283
4. Boris, J.P. and Book, D.L. (1976): Flux corrected transport. III. Minimal error FCT algorithms. *J. Comp. Phys.* **20**, pp. 397-431

5. Breuß, M. (2004): The correct use of the Lax-Friedrichs method. *RAIRO Math. Models Num. Anal.* **38**, No. 3, pp. 519-540
6. Evans, L. (1998): *Partial Differential Equations*. American Mathematical Society
7. Gilboa G., Sochen, N.A., and Zeevi Y.Y. (2002): Forward-and-backward diffusion processes for adaptive image enhancement and denoising. *IEEE Trans. Image Proc.* **11**, No. 7, pp. 689-703
8. Godlewski, E. and Raviart, P.-A. (1991): *Hyperbolic Systems of Conservation Laws*. Ellipses, Edition Marketing
9. Godlewski, E. and Raviart, P.-A. (1996): *Numerical Approximation of Hyperbolic Systems of Conservation Laws*. Springer, New York
10. Grahns, T., Meister, A., and Sonar T. (2002): Image processing for numerical approximations of conservation laws: nonlinear anisotropic artificial dissipation. *SIAM J. Sci. Comp.* **23**, No. 5, pp. 1439-1455
11. Grahns, T. and Sonar T. (2002): Entropy-controlled artificial anisotropic diffusion for the numerical solution of conservation laws based on algorithms from image processing. *J. Visual Commun. Image Repr.* **13**, No. 1/2, pp. 176-194
12. LeFloch, P.G. and Liu, J.-G. (1999): Generalized monotone schemes, discrete paths of extrema, and discrete entropy conditions. *Math. Comp.*, **68**, No. 227, pp. 1025-1055
13. LeVeque, R.J. (1992): *Numerical Methods for Conservation Laws*. Birkhäuser, 2nd Edition
14. Osher, S. and Rudin, L. (1990): Feature-oriented image enhancement using shock filters. *SIAM J. Num. Anal.* **27**, pp. 919-940
15. Osher, S. and Rudin, L. (1991): Shocks and other nonlinear filtering applied to image processing. *SPIE Vol. 1567: Applications of Digital Image Processing XIV*, pp. 414-425
16. Perona, P. and Malik, J. (1990): Scale space and edge detection using anisotropic diffusion. *IEEE Trans. Pattern Anal. Mach. Intell.*, **12**, pp. 629-639
17. Pollak, I., Willsky, A.S., and Krim, H. (2000): Image segmentation and edge enhancement with stabilized inverse diffusion equations. *IEEE Trans. Image Proc.* **9**, No. 2, pp. 256-266
18. Rudin, L.I. (1987): *Images, Numerical Analysis of Singularities and Shock Filters*. Ph.D. thesis, California Institute of Technology, Pasadena, CA
19. Rudin, L.I., Osher, S., and Fatemi, E. (1992): Nonlinear total variation based noise removal algorithms. *Physica D* **60**, pp. 259-268
20. Roe, P.L. (1981): *Numerical algorithms for the linear wave equation*. Technical Report 81047, Royal Aircraft Establishment, Bedford, UK
21. Sweby, P.K. (1984): High resolution schemes using flux limiters for hyperbolic conservation laws. *SIAM J. Num. Anal.* **21**, pp. 995-1011
22. Wei, G.W. (2002): Shock capturing by anisotropic diffusion oscillation reduction. *Comp. Phys. Commun.* **144**, pp. 317-342
23. Weickert, J. (1998): *Anisotropic Diffusion in Image Processing*. Teubner, Stuttgart.
24. Zalesak, S.T. (1997): Introduction to "Flux corrected transport. I. SHASTA, a fluid transport algorithm that works". *J. Comp. Phys.* **135**, pp. 170-171